Ceramide-Domain Formation and Collapse in Lipid Rafts: Membrane Reorganization by an Apoptotic Lipid

Liana C. Silva,* Rodrigo F. M. de Almeida,*† Bruno M. Castro,* Alexander Fedorov,* and Manuel Prieto*
*Centro de Química-Físcia Molecular, Instituto Superior Técnico, Lisbon, Portugal; and †Departamento de Química e Bioquímica, Faculdade de Ciências da Universidade de Lisboa, Lisbon, Portugal

ABSTRACT The effect of physiologically relevant ceramide concentrations (≤4 mol %) in raft model membranes with a lipid composition resembling that of cell membranes, i.e., composed of different molar ratios of an unsaturated glycerophospholipid, sphingomyelin, and cholesterol (Chol) along a liquid-disordered-liquid-ordered tie line was explored. The application of a fluorescence multiprobe and multiparameter approach, together with multiple fluorescence resonance energy transfer (FRET) pairs, in the well-characterized palmitoyl-oleoyl-phosphocholine (POPC)/palmitoyl-sphingomyelin (PSM)/Chol ternary mixture, revealed that low palmitoyl-ceramide (PCer) concentrations strongly changed both the biophysical properties and lipid lateral organization of the ternary mixtures in the low-to-intermediate Chol/PSM-, small raft size range (<25 mol % Chol). For these mixtures, PCer recruited up to three PSM molecules for the formation of very small (~4 nm) and highly ordered gel domains, which became surrounded by rafts (liquid-ordered phase) when Chol/PSM content increased. However, the size of these rafts did not change, showing that PCer did not induce the formation of large platforms or the coalescence of small rafts. In the high Chol/PSM-, large raft domains range (>33 mol % Chol), Chol completely abolished the effect of PCer by competing for PSM association. Lipid rafts govern the biophysical properties and lateral organization in these last mixtures.

INTRODUCTION

At the present time, the plasma membrane is considered to be a dynamic entity, where specific lipid-lipid interactions occur, leading to the formation of organized structures (the so-called lipid domains) that coexist in biomembranes (1). In the last decades, several studies were directed to the membrane structure and, in particular, to the lipid-lipid interactions and lipid organization into membrane domains (2). Cholesterol (Chol), for example, has received special attention due to its condensing effect on the liquid-crystalline phase, its ability in fluidizing the gel phase and in promoting fluid-fluid phase separation in several lipid bilayers (e.g, (3–7)). Membrane rafts are a specific type of lipid domains, sphingolipid- and Chol-enriched, that result from tight hydrophobic interactions between these molecules leading to the spontaneous formation of aggregates that separate from glycerophospholipids in cell membranes (8). Due to their lipid composition, rafts are assumed to exist in a more ordered state (the liquid-ordered phase, l_o) than the bulk membrane where the lipids are in a liquid-disordered (l_d) phase. Several studies suggest that sphingolipids and rafts play a role in a variety of cellular processes, such as cell signaling, endocytosis, lipid and protein sorting, and organization and membrane trafficking (9,10). Many proteins involved in signal cascades require the presence of intact lipid rafts for their activation. The distinct biophysical properties of rafts lead to the hypothesis that the membrane physical state could be the cause of the activation/inhibition of cellular processes (11,12). Sphingomyelin (SM) is the most abundant sphingolipid and is composed of a hydrophobic ceramide (Cer) backbone and a hydrophilic phosphorylcholine headgroup. SM is predominantly located in the outer leaflet of the cell membrane, and it is estimated that 70% of total SM is found in lipid rafts (13).

Recently it was proposed that rafts are the primary site of action of the enzyme sphingomyelinase (SMase) that catalyzes the hydrolysis of SM resulting in Cer formation. It was also proposed that upon enzymatic Cer generation, rafts would merge into large platforms that would serve as the site for signal transduction initiation by driving the clustering of several receptors and proteins of a given signalosome (for review, see Gulbins et al. (14) and Bollinger and Teichgraber (15)). Due to its unique biophysical properties and its high tendency to spontaneously associate into membrane domains (12), the generation of Cer per se is usually considered to be sufficient to drive the fusion of small rafts into large platforms (16). Studies in fluid model membranes have shown that Cer is able to drive the formation of gel domains that segregate from the fluid lipids (17–19). Moreover, increasing Cer concentration leads not only to the formation of large and highly ordered Cer platforms, but also to morphological alterations in the vesicles, including aggregation, vesiculation, and tubular structure formation (20). In addition, it was suggested that in the presence of Chol, Cer would selectively displace Chol from rafts, competing for association with the other lipids (21). Studies in SM/Cer gel model membranes show that Cer is able to segregate from SM into Cer-rich and -poor domains (22).

However, the effect of Cer in raft model membranes with a lipid composition resembling that of cell membranes, i.e., composed of an unsaturated glycerophospholipid, SM and Chol is still poorly studied. In this study, we explore the

Submitted June 23, 2006, and accepted for publication September 28, 2006.

Address reprint requests to Liana C. Silva, Centro de Química-Física Molecular, Instituto Superior Técnico, Av. Rovisco Pais, 1049-001 Lisboa, Portugal, Fax: 351-218-464-455; E-mail: lianacsilva@ist.utl.pt.

0006-3495/07/01/502/15 $2.00

doi: 10.1529/biophysj.106.091876

biophysical properties of a well-defined raft-model mixture: 1-palmitoyl-2-oleoyl-*sn*-glycero-3-phosphocholine (POPC)/*N*-palmitoyl-sphingomyelin (PSM)/Chol- in the presence of low *N*-palmitoyl-Cer (PCer) amounts. The ternary system was extensively characterized both in phase behavior (23) and raft size variation (24) as a function of lipid composition, allowing us to accurately describe the Cer-induced biophysical changes in rafts with different size and composition (the relation between lipid composition and raft size variation is shown in Fig. 1). The application of a previously developed multiprobe approach (20), now adding multiple fluorescence resonance energy transfer (FRET) pairs, allowed us to determine changes in acyl chain order, to detect PCer/PSM gel-domain formation and quantify their fraction, composition, and size, and to study PCer-induced lateral lipid reorganization in raft-forming membranes as a function of lipid composition (namely, Chol content). Our results show that PCer strongly affects both membrane biophysical properties and lipid lateral organization only in rafts presenting low-to-intermediate Chol/PSM content, i.e., in the small raft size range.

MATERIALS AND METHODS

Materials

POPC, PCer, PSM, Rho-DOPE (1,2-Dioleoyl-*sn*-Glycero-3-Phosphoethanolamine-*N*-(Lissamine Rhodamine B Sulfonyl)) and NBD-DOPE (1,2-Dioleoyl-*sn*-Glycero-3-Phosphoethanolamine-*N*-(7-nitro-2-1,3-benzoxadiazol-4-yl)) were obtained from Avanti Polar Lipids (Alabaster, AL). DPH (1,6-diphenyl-1,3,5-hexatriene), NBD-DPPE (1,2-Dipalmitoyl-*sn*-Glycero-3-Phosphoethanolamine-N-(7-nitro-2-1,3-benzoxa-diazol-4-yl)) and t-PnA (*trans*-parinaric acid) were from Molecular Probes (Leiden, The Netherlands). Chol was from Sigma (St. Louis, MO). All organic solvents were UVASOL grade from Merck (Darmstad, Germany).

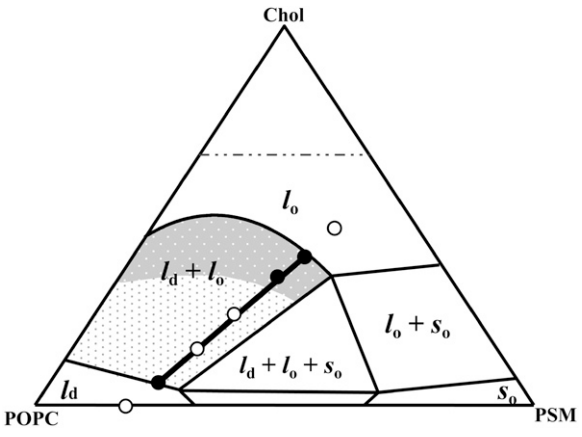

FIGURE 1 Ternary phase diagram of POPC/PSM/Chol mixtures (adapted from de Almeida et al. (24)). The black line corresponds to the tie line that contains the 1:1:1 POPC/PSM/Chol mixture. The black dots in the tie line define this composition and the extremes of the tie line. The POPC/PSM/Chol ratios for the mixtures used in this study were taken from this tie line and are represented by the white dots. The gray shades represent regions of different sized raft domains: in the low-to-intermediate Chol/PSM range (*light gray*) raft domains are small (ranging from <20 to ~75 nm), whereas in the high Chol/PSM range (*dark gray*) larger rafts are formed (>~100 nm).

Liposome preparation

Multilamellar vesicles (MLV) (total lipid concentration 0.1 mM) containing the adequate lipids and probes were prepared as previously described (20). The suspension medium was sodium phosphate 10 mM, NaCl 150 mM, EDTA 0.1 mM buffer (pH 7.4). The samples were reequilibrated by freeze-thaw cycles, incubated at $T > 90°C$, and subsequently kept overnight at 4°C. Before starting the measurements, the samples were slowly heated to the required temperature and incubated for at least 1 h. The probe to lipid (P/L) ratio used was 1:200 for DPH and 1:500 for t-PnA. The mol fractions of each component PSM, POPC, and Chol were selected to span the tie line containing the 1:1:1 equimolar mixture taken from the ternary POPC/PSM/Chol phase diagram (23) (for the sake of clarity both the ternary diagram and this tie line are present in Fig. 1), i.e., they are linear combinations of the terms defining the composition of each coexisting phase (extremes of the tie line), where the coefficients (between 0 and 1) are X_{lo} and $1 - X_{lo} = X_{ld}$ (X_i is phase or component i mol fraction). Additionally, two more mixtures with a lipid composition that is still defined by this line but that lay outside the extremes of the tie line (i.e., in the l_d and in the l_o region of the ternary phase diagram) were also selected to better define the trend of variation of the different parameters with the composition of the system. The ternary mixtures used in this study were 78.3:21.7:0; 71.6:23.3:5; 59.7:26.3:14; 45.1:29.9:25; 34:32.7:33.3; 25.4:34.8:39.8; and 15.1:37.4:47.5 POPC/PSM/Chol (see Fig. 1). The concentration of POPC, PSM, Chol, and PCer stock solutions was determined gravimetrically with a high precision balance (Mettler Toledo UMT2). Probe concentrations were determined spectrophotometrically using ε(t-PnA, 299.4 nm, ethanol) = 89×10^3 $M^{-1}cm^{-1}$ (25), ε(DPH, 355 nm, chloroform) = 80.6×10^3 $M^{-1}cm^{-1}$ (26), ε(NBD-DOPE or DPPE, 458 nm, chloroform) = 21×10^3 $M^{-1}cm^{-1}$, and ε(Rho-DOPE, 559 nm, chloroform) = 95×10^3 $M^{-1}cm^{-1}$ (27).

Absorption and fluorescence

All measurements were performed in 0.5 cm × 0.5 cm quartz cuvettes and under magnetic stirring. The absorption and steady-state fluorescence instrumentation was previously described (28). The absorption spectra were corrected for turbidity. For steady-state fluorescence measurements, the excitation (λ_{exc})/emission (λ_{em}) wavelengths were 358/430 nm for DPH; 303/405 nm for t-PnA; 465/536 nm for NBD-DOPE and NBD-DPPE; and 570/593nm for Rho-DOPE. The temperature was achieved by a Julabo F25 circulating water bath and controlled with 0.1°C precision directly inside the cuvette with a thermocouple. For measurements performed at different temperatures, the heating rate was always below 0.2°C/min.

The time-resolved fluorescence measurements with t-PnA were performed using λ_{exc} = 295nm (secondary laser of Rhodamine 6G (23)) and λ_{em} = 405 nm. For NBD-DOPE and NBD-DPPE λ_{exc} = 428 nm (Ti-Sapphire laser, (24)) and λ_{em} = 536 nm were used. The data were analyzed as previously described (28). For a decay described by a sum of exponentials where α_i is the normalized preexponential and τ_i is the lifetime of the decay component i, the lifetime-weighted quantum yield and the mean fluorescence lifetime are given by: $\bar{\tau} = \sum_i \alpha_i \tau_i$ and $\langle\tau\rangle = \sum_i \alpha_i \tau_i^2 / \sum_i \alpha_i \tau_i$, respectively.

Determination of the partition coefficients of the probes between different phases and phase mol fraction

The partition coefficient of the probes between l_o and l_d, $K_p^{lo/ld}$, and between gel and fluid phases, $K_p^{g/f}$, were determined from the variation of the photophysical parameters of the probes with the molar fraction of l_o phase, X_{lo}, and gel phase, X_G, respectively. To accurately describe the partition of the probes between the phases under study, ternary mixtures of POPC/PSM/Chol and binary mixtures of POPC/Cer were used to determine the partition toward an l_o phase composed of (mainly) PSM/Chol and to a gel phase composed of (mainly) PCer, respectively. The composition of the mixtures

and the molar fraction of each phase were taken from the tie lines of the respective phase diagram (20,24). This methodology allows for determining a constant that truly represents the partition of the probes toward the specific phases under study (e.g., a gel-phase containing PCer excludes probes that usually are able to partition into a phospholipid gel phase) and consequently is independent of the particular composition of the mixtures. Note that the extent of the partition depends on the amount of each phase, but the partition coefficient is independent because the determination of this constant is made along a tie line where the composition of each phase remains the same.

When no significant spectral shifts occur, the partition coefficient is calculated according to the following expressions (29):

i. from lifetime-weighted quantum yield, $\bar{\tau}$,

$$\bar{\tau} = \frac{\bar{\tau}_1 K_p X_1 + \bar{\tau}_2 X_2}{K_p X_1 + X_2}, \quad (1)$$

ii. from mean fluorescence lifetime, $\langle\tau\rangle$,

$$\langle\tau\rangle = \frac{\langle\tau\rangle_1 K_p X_1 + \bar{\tau}_2/\bar{\tau}_1\langle\tau\rangle_2 X_2}{K_p X_1 + \bar{\tau}_2/\bar{\tau}_1 X_2}, \quad (2)$$

iii. from steady-state fluorescence intensity, I_F,

$$I_F = \frac{K(\varepsilon_1\phi_1 K_p X_1 + \varepsilon_2\phi_2 X_2)}{(K_p X_1 + X_2)}, \quad (3)$$

iv. from steady-state fluorescence anisotropy, $\langle r\rangle$,

$$\langle r\rangle = \frac{\varepsilon_1\phi_1 r_1 K_p X_1 + \varepsilon_2\phi_2 r_2 X_2}{\varepsilon_1\phi_1 K_p X_1 + \varepsilon_2\phi_2 X_2}, \quad (4)$$

where $1 = l_o$ or gel and $2 = l_d$ or fluid, K is a normalization factor that accounts for the arbitrary units of fluorescence intensity, ε_i is the molar absorption coefficient, ϕ_i the quantum yield, $\langle\tau\rangle_i$, $\bar{\tau}_i$, and r_i are the mean fluorescence lifetime, the lifetime-weighted quantum yield, and steady-state fluorescence anisotropy of the probe in phase i, respectively. K_p is obtained by fitting the equations to the data as a function of X_i. Conversely, these equations can be used to determine X_i in a given sample if the parameter in question and the K_p are known for the pure coexisting phases.

FRET experiments

To avoid multilayer geometry, FRET experiments were carried out in large unilamellar vesicles (LUV) (1 mM total lipid concentration), obtained from MLV by the extrusion technique (24). Donor and acceptor (D/A) pairs were chosen in accordance to their phase-related properties to characterize the following situations: i) NBD-DPPE/Rho-DOPE for FRET between l_o and l_d phases. The P/L ratios were 1/1000 and 1/200, respectively. For this donor P/L ratio, no self-quenching nor energy homotransfer take place (29); ii) t-PnA/NBD-DOPE for FRET between gel and fluid (both l_o and l_d) phases; and iii) t-PnA/NBD-DPPE for FRET between gel and l_o. The P/L ratio was 1/1000 for t-PnA, 1/250 for NBD-DOPE and 1/100 for NBD-DPPE. Data analysis was carried out as described (24) (see Appendix for the detailed model). FRET efficiency, E, was obtained from the time-resolved fluorescence intensity curves, through the relation $E = 1 - \bar{\tau}_{DA}/\bar{\tau}_D$.

RESULTS

Phase behavior of the probes

In this study, the composition of the ternary mixtures was taken from the tie line at 23°C that contains the 1:1:1 POPC/PSM/Chol mixture in the ternary phase diagram (23). In this situation, model rafts are always formed (this tie line lies in the region that corresponds to the $l_o - l_d$ phase coexistence of the diagram), and their size increases with the Chol/PSM content of the mixtures (see Fig. 1) (24). To evaluate the changes induced by PCer in the raft model systems, several fluorescent probes with different phase-related properties were used. In a previous work (20) we have shown that t-PnA is the best probe to report the properties of PCer-rich domains, due to the highly ordered nature of these domains that exclude other probes. A multiprobe approach was required to unravel the complexity of the simple binary POPC/PCer mixtures. The full characterization of the more complex mixtures is only possible by applying this methodology. The comparison of the fluorescence properties between the probes can only be made by taking into consideration their preferential partition between different phases. In this way, the partition coefficients between l_o and l_d, $K_p^{lo/ld}$, and gel and fluid, $K_p^{g/f}$, phases were determined toward the phases under study, i.e., l_o PSM/Chol-enriched and gel Cer-enriched. The values obtained and the methodologies used are listed in Table 1. A probe that prefers an l_o or a gel phase (in l_o/l_d and gel/fluid phase separation, respectively) presents a $K_p > 1$, whereas a preferential partition to a l_d or a fluid phase leads to a $K_p < 1$.

Note that the value obtained corresponds to an equilibrium constant and thus it will be independent on the composition of the mixtures along the tie line. If different phases are present in the mixtures, the distribution of the probes will be described by all the partition coefficients. The ability of different probes to distribute differentially between the phases allows studying the lipid lateral distribution in the membrane. The values presented in Table 1 clearly indicate that t-PnA strongly partitions to a PCer-rich gel phase, whereas the other probes are excluded from this gel. Among fluid phases, NBD-DPPE has a strong preference for the PSM/Chol-rich l_o phase, whereas Rho-DOPE strongly prefers the POPC-rich l_d phase. All the other probes distribute almost evenly between these fluid phases.

TABLE 1 Partition coefficients of the probes between l_o and l_d, $K_p^{lo/ld}$, and gel and fluid, $K_p^{g/f}$, phases

Probe	$K_p^{lo/ld}$ in POPC/PSM/Chol	$K_p^{g/f}$ in POPC/PCer
DPH	1.05 ± 0.08*	~0*§
NBD-DOPE	1.20 ± 0.06†	~0†§
NBD-DPPE	3.68 ± 0.55†	~0†§
Rho-DOPE	0.28 ± 0.08‡	~0‡§
t-PnA	0.88 ± 0.05†	4.50 ± 0.60†

*K_p was determined from Eq. 4.
†K_p was determined from Eq. 1.
‡K_p was determined from Eq. 3.
§The photophysical parameters of these probes remain almost unchanged, with PCer-gel fraction indicating that their partition into the PCer-gel phase is very low.

PCer strongly perturbs membrane order and lipid distribution

Fig. 2 *A* shows the fluorescence anisotropy, $\langle r \rangle$, of DPH and t-PnA as a function of Chol mol fraction, X_{Chol}, for the ternary mixtures (varying the molar ratio of the three components POPC/PSM/Chol along the tie line) containing 0, 2, or 4 mol % of PCer. In the absence of PCer (*circles*), the anisotropy of both DPH and t-PnA sharply increased with X_{Chol}, reporting the formation of l_o phase. However, whereas the presence of PCer leads only to a slight increase in the anisotropy of DPH, it markedly changed the trend of variation observed for t-PnA. For low-to-intermediate X_{Chol}, which corresponds to the small raft-size range (Fig. 1), t-PnA anisotropy sharply increased with PCer content, showing that PCer induced the formation of a more ordered phase that does not affect DPH anisotropy. Increasing X_{Chol} abolished the effect of PCer, indicating that Chol and PCer compete for PSM association, as previously suggested for natural and synthetic Cer in other lipid mixtures (21). An interesting observation was that, similarly to what was observed for higher Cer amounts in POPC/PCer mixtures (20), DPH is unable to report the changes induced by low PCer amounts in the raft mixtures, suggesting that in the presence of other lipid components physiological levels of Cer are able to drive the formation of highly ordered domains that exclude DPH. As will be clear later, these domains correspond to PCer/PSM-rich gel domains. It should be stressed that the effect of only 2 or 4 mol % of PCer in the low Chol regime for the ternary mixtures is similar to the one obtained for 4 and 12 mol %, respectively, in the binary POPC/PCer mixtures (20) and thus to a gel-fluid boundary and to a clear gel-fluid phase coexistence, respectively, in this binary phase diagram.

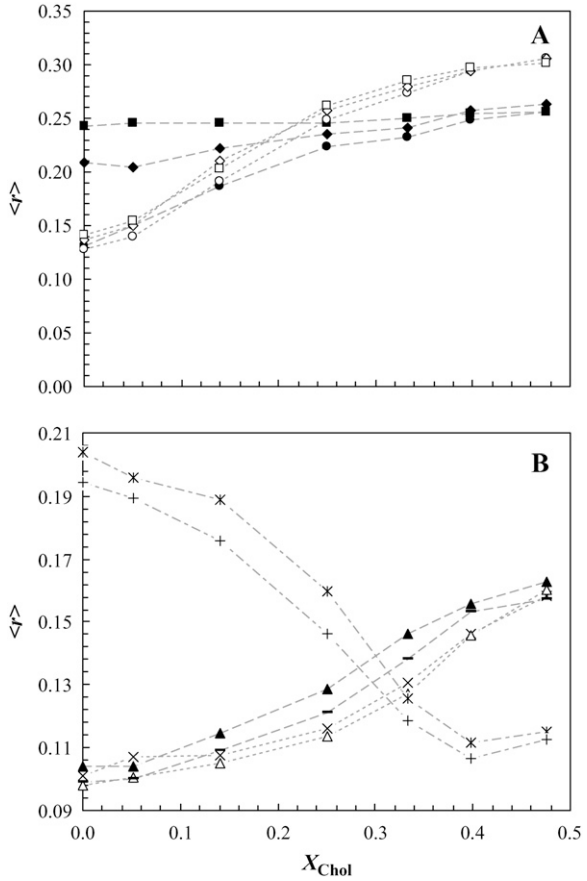

FIGURE 2 Effect of low PCer amounts on the fluorescence anisotropy of the probes in the ternary mixtures. (*A*) t-PnA (*solid symbols*) and DPH (*open symbols*) anisotropy in ternary mixtures containing 0 (*circles*), 2 (*diamonds*), and 4 (*squares*) mol % PCer. (*B*) Anisotropy of Rho-DOPE (*,+), NBD-DPPE (−,▲), and NBD-DOPE (×,△) for ternary mixtures containing 0 and 4 mol % PCer, respectively. The lines are merely a guide to the eye. The error bars are within the size of the symbol and correspond to at least five independent measurements.

NBD-DPPE and NBD-DOPE were also used to study the effects of PCer in the ternary mixtures. Fig. 2 *B* shows the variation of the anisotropy of these probes for 0 and 4 mol % PCer with X_{Chol}. In the absence of PCer the anisotropy of both probes increases with X_{Chol}, reporting the formation of l_o phase. Note that, for the lowest and highest Chol concentrations, $\langle r \rangle_{NBD\text{-}DPPE} \sim \langle r \rangle_{NBD\text{-}DOPE}$, whereas for the intermediate Chol concentrations $\langle r \rangle_{NBD\text{-}DPPE}$ is slightly higher. This is due to a higher partition of the NBD-DPPE probe into the l_o phase ($K_p^{lo/ld} \sim 3.7$) as compared to NBD-DOPE ($K_p^{lo/ld} \sim 1.2$). The anisotropy values of NBD-DPPE slightly increased in the presence of PCer reporting an increase in rigidity. In contrast, NBD-DOPE anisotropy decreased suggesting that the probe is excluded from the PCer-rich regions. Due to the presence of an unsaturation in the lipid chain of this probe, it has a higher tendency to segregate to more fluid regions. As a result, its surface concentration increases leading to depolarization by energy homotransfer (30).

The anisotropy observed for Rho-DOPE (Fig. 2 *B*) presents a completely different trend of variation, even in the absence of PCer, strongly decreasing with X_{Chol}. This is due to an efficient energy homotransfer between Rho-DOPE molecules that leads to a strong emission depolarization (24). In the presence of PCer the depolarization is even higher, suggesting that the local concentration of the probe in the fluid phase is higher due to its exclusion from PCer-rich domains.

The fluorescence lifetimes of the probes are reliable reporters of the lipid phases

To determine the nature of PCer-rich regions, the fluorescence intensity decay of t-PnA was measured. The appearance of a long lifetime component in t-PnA fluorescence decay that leads to a sharp increase in the mean fluorescence lifetime of the probe is a reporter of the formation of PCer-gel domains (20). t-PnA presents a complex decay, described by the sum of three or four exponentials depending on the composition of the mixtures. For the ternary mixtures in the absence of PCer, three exponentials were required to describe

the probe's fluorescence decay. The formation of l_o phase is reported by the increase in τ_3 (from ~5 to 25 ns) with X_{Chol} (Fig. 3 *A*). In the presence of 2 mol % PCer, τ_3 is higher for the low-to-intermediate Chol regime (~30 ns) and tends to the values obtained in the absence of PCer when $X_{Chol} > 25$ mol % (Fig. 3 *B*), reporting the opposite effects of PCer and Chol on the biophysical properties of the lipid mixtures. For $X_{Cer} = 4$ mol % and in the low-to-intermediate Chol regime, four exponentials were required to describe the decay of the probe (Fig. 3 *C*). This new long lifetime component (~50 ns) clearly reports the formation of a gel phase (20). For $X_{Chol} >$ 25 mol % the fluorescence decay of t-PnA is again described by three exponentials (identical to those obtained for 0 mol % PCer), showing that Chol is able to abolish the gel phase. Note that although both PSM and Chol mol fraction increase along the tie line studied, we can clearly conclude that Chol is the molecule abolishing the gel domains because, in the absence of POPC and Chol, PSM is in the gel phase at room temperature.

The mean fluorescence lifetime is a parameter highly sensitive to the presence of a long component on the fluorescence decay. Due to the difficulty in attributing the shorter components to a specific phase (28), representing the mean lifetime of t-PnA as a function of X_{Chol} is the most illustrative way of showing the effects of PCer on the lipid raft model system. The values obtained for 4 mol % PCer (Fig. 4 *A*) are typical of a gel phase and comparable to those obtained for binary POPC/PCer mixtures containing ~12 mol % PCer (20). Increasing X_{Chol} leads to a decrease in the mean fluorescence lifetime of the probe down to values typical of l_o phase and close to the ones measured in the absence of PCer. For 2 mol % PCer the increase of the mean fluorescence lifetime is not so pronounced and the values indicate that only an ordering effect induced by PCer is occurring in the fluid mixture. Similarly to the changes observed in the anisotropy, this variation is comparable to the effect of 4% Cer in the POPC/PCer mixture, and thus to the boundary that separates the fluid from the gel-fluid phase coexistence region in this binary phase diagram (20). In this situation, it is expected that the variations in the mean fluorescence lifetime of t-PnA are not so steep because only a very small fraction of gel phase, if any, is present.

For the NBD-labeled lipids, the lifetime-weighted quantum yield increases with X_{Chol} sensing the formation of l_o phase (Fig. 4 *B*). However, it decreases for both probes in the presence of PCer. This is explained by an efficient self-quenching (30) due to an increased surface density of the probes that are excluded from the PCer-rich domains. It is interesting to note that even with a higher lifetime, NBD-DPPE presents a slightly higher anisotropy, compared to NBD-DOPE, for the samples with $l_d + l_o$ coexistence. Since the effect of a higher lifetime is a lower anisotropy (Perrin equation, e.g., (31)) the differences between the anisotropy of both probes are significant and due to a different partition coefficient.

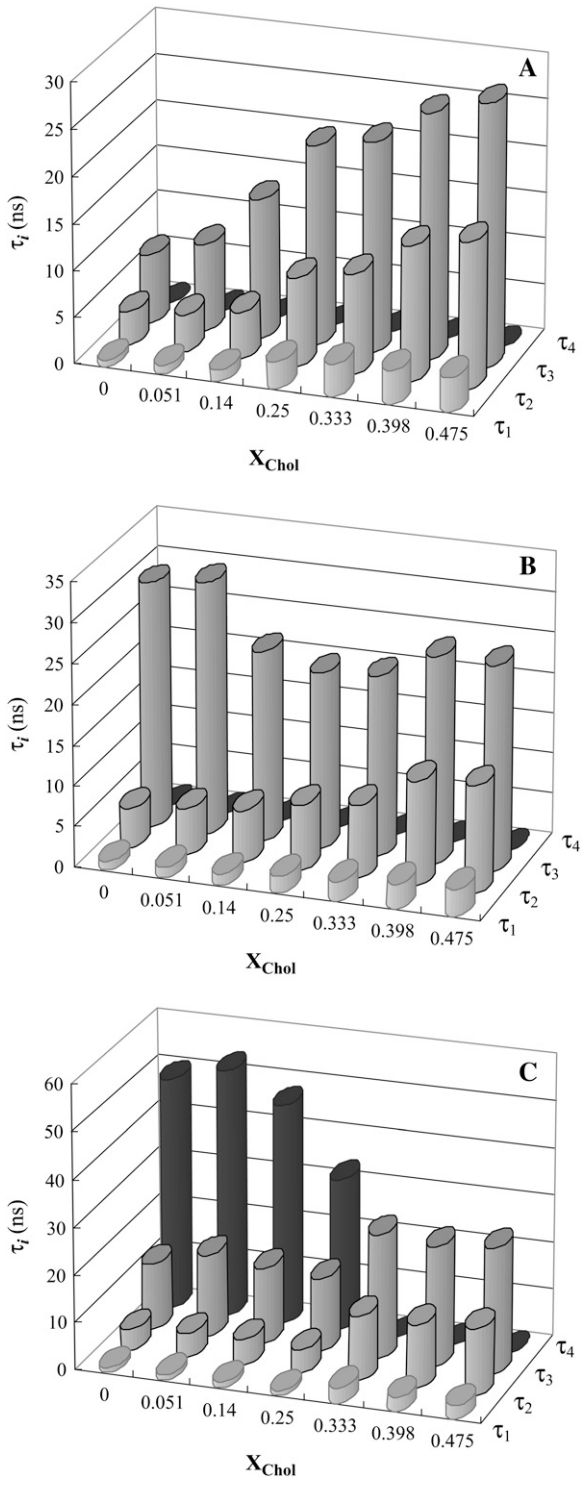

FIGURE 3 Variation of the lifetime components of t-PnA fluorescence decay with lipid composition for the ternary POPC/PSM/Chol mixtures along the tie line that crosses the 1:1:1 mixture at room temperature containing (*A*) 0, (*B*) 2, and (*C*) 4 mol % PCer.

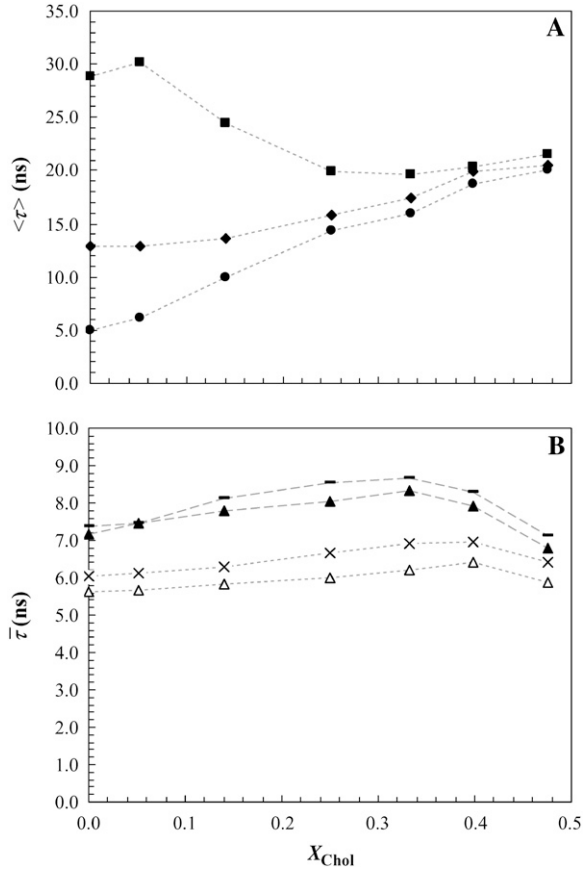

FIGURE 4 Effect of PCer on the fluorescence lifetime of the probes. (*A*) Mean fluorescence lifetime of t-PnA in the ternary mixtures containing 0 (*circles*), 2 (*diamonds*), and 4 (*squares*) mol % PCer. (*B*) Lifetime-weighted quantum yield of NBD-DPPE (−,▲) and NBD-DOPE (×,△) in ternary mixtures containing 0 and 4 mol % PCer, respectively. The dotted lines are only a guide to the eye.

Effect of PCer on the thermotropic properties of rafts mixtures

To investigate the effect of PCer on the thermotropic properties of the ternary mixtures, the anisotropy of t-PnA was measured as a function of temperature (Fig. 5). For the low Chol/PSM regime (Fig. 5 *A*) t-PnA is able to detect the gel-fluid phase transition of PSM-enriched domains, which is shifted toward higher temperatures in a PCer-concentration-dependent manner ($T_m \sim 36$ and 47°C for 2 and 4 mol % Cer, respectively). Note that this does not correspond to a true T_m because there is phase coexistence along a range of temperatures. It corresponds to a mean value indicative of the thermal stability of gel domains. Upon increasing Chol content (Fig. 5 *B*), the gel-fluid phase transition of PSM-enriched domains becomes less and less pronounced due to the presence of l_o phase. However, when in the presence of PCer, the gel-fluid phase transition was again steeper, showing that PCer interacts with PSM in an opposite manner to Chol, stabilizing the gel domains. For Chol concentrations where

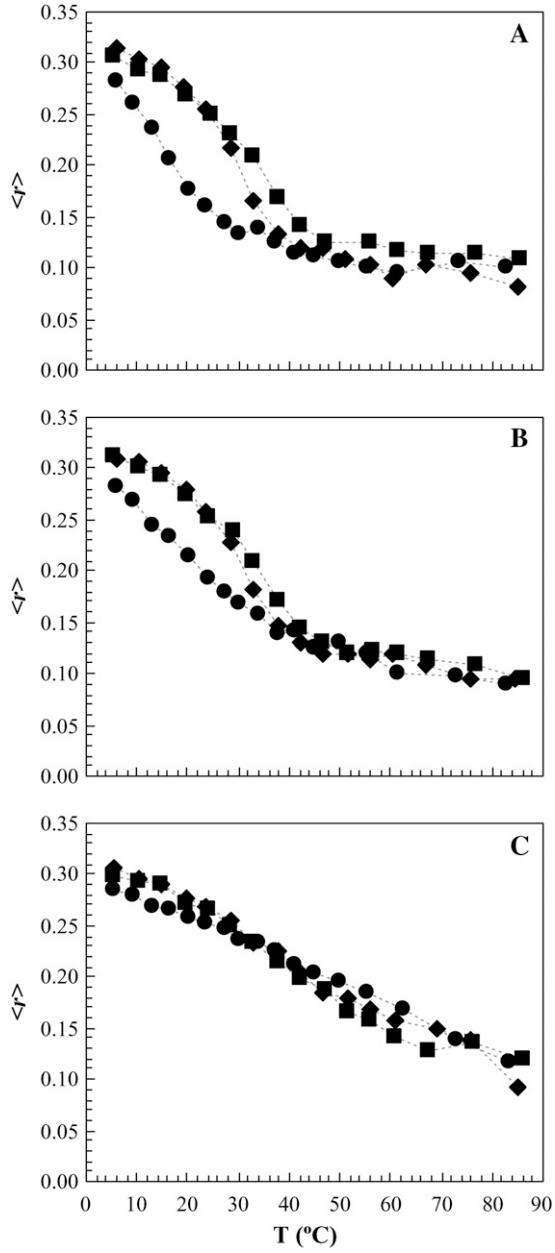

FIGURE 5 Variation of t-PnA fluorescence anisotropy with temperature for (*A*) POPC/PSM/Chol: 0.72:0.23:0.05 molar ratio, (*B*) POPC/PSM/Chol: 0.60:0.26:0.14 molar ratio, and (*C*) POPC/PSM/Chol: 0.25:0.35:0.40 molar ratio, containing 0 (*circles*), 2 (*diamonds*), and 4 (*squares*) mol % PCer. The dotted lines are only a guide to the eye. The T_m was taken by the midpoint of the intersection of the lines describing the initial (gel), intermediate (gel and fluid), and final (fluid) regimes (see de Almeida et al. (23) for additional details).

only the l_o phase is present in the ternary mixtures (Fig. 5 *C*), t-PnA anisotropy was practically independent of PCer content, showing that Chol completely abolished the PCer effect. These results further support the hypothesis that Chol and PCer are competing for PSM and modulating the membrane biophysical properties in opposite ways.

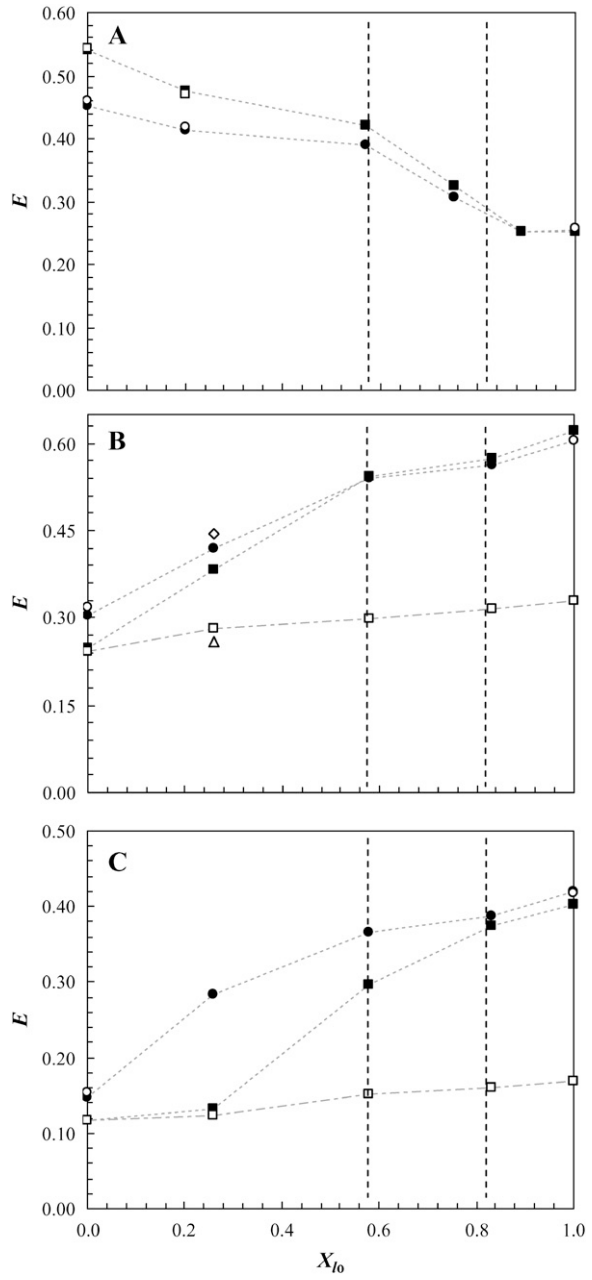

FIGURE 6 Variation of FRET efficiency, E, for the donor/acceptor pair (*A*) NBD-DPPE/Rho-DOPE, (*B*) t-PnA/NBD-DPPE, and (*C*) t-PnA/NBD-DOPE as a function of l_o molar fraction, X_{lo}, in the $l_o + l_d$ coexistence region along the tie line of the ternary phase diagram for the POPC/PSM/Chol mixture (24) containing 0 (*circles*) and 4 (*squares*) mol % PCer. Experimental data are represented by solid symbols, and open symbols are values from theoretical calculations. The open circles were obtained by calculation of the expected E for a random distribution of donors and acceptors. The open squares correspond to (*A*) the expected E in a situation where surface area for probe distribution decreases due to formation of gel domains that exclude both donor and acceptors, and (*B*,*C*) the expected E when donors located both in the gel and fluid phases are transferring energy to acceptors randomly distributed in the fluid phases. In these calculation $X_G = 15\%$ and a $R_e = 3.8$ and 4.0 nm for NBD-DPPE and NBD-DOPE, respectively, were assumed (see Discussion and Appendix for further details). The open triangle and the open diamond (*B*) correspond to the expected E for a situation where PCer/PSM gel domains are surrounded by only l_d or l_o phases, respectively. It was assumed that donors located in the gel phase were only able to transfer to one of the fluid phases, $X_G = 15\%$, $R_e = 3.8$, and the amount of donor in the gel phase and the surface density of the acceptors in each fluid phase was taken into account (see Appendix for further details). The dotted and dotted-dashed lines are only to guide the eye. The vertical dashed lines correspond to the mixtures containing 25% and 33% Chol. Time-resolved FRET measurements are extremely reproducible, and variations in the values of E are within $<1.5\%$ for completely independent samples.

PCer changes the lateral organization of membranes containing rafts

The FRET efficiency, E, between a donor and an acceptor which preferentially partition into different phases is a reliable method to estimate the size of lipid domains in the nanometer range (20,24). As shown above, the presence of PCer in the ternary mixtures strongly perturbs the biophysical properties of the rafts, and an attempt to estimate the extent of the perturbation can only be based on the combination of E variations obtained for the different phases using multiple donor and acceptor pairs. Based on the K_p of the several probes (Table 1) the following D/A pairs were used: i) NBD-DPPE/Rho-DOPE; ii) t-PnA/NBD-DPPE; and iii) t-PnA/NBD-DOPE to study the perturbations induced by PCer in the l_o/l_d, gel/l_o, and gel/fluid (both l_o and l_d) interactions, respectively (Fig. 6). The system under study is very complex, and the quantitative methodology applied by us to determine the size of the rafts (24) and Cer-platforms (20), where E along a tie line is used cannot be applied in the present case because PCer changes the tie line (see Fig. 7) and in most mixtures three phases are present (see Discussion). However, relevant topological information can be obtained and quantification is possible using an alternative approach.

Fig. 6 clearly shows different trends of FRET efficiencies for the several D/A pairs used which are reflecting the changes in the lateral lipid distribution. It was observed that for the low-to-intermediate l_o molar fraction, X_{lo}, range (i.e., $X_{Chol} < 25$–33 mol %): i) E between NBD-DPPE and Rho-DOPE increases with 4% PCer (Fig. 6 *A*). This increase is due to an exclusion of the probes from gel regions (both probes preferentially partition into fluid phases) and thus to a closer distribution of both probes in the fluid phases; ii) E between t-PnA and NBD-DPPE (Fig. 6 *B*) decreases in the presence of PCer due to the formation of gel domains; and iii) E between t-PnA and NBD-DOPE (Fig. 6 *C*) strongly decreases with 4% PCer. Because the acceptor chromophore is the same in t-PnA/NBD-DPPE and t-PnA/NBD-DOPE pairs, the higher decrease observed for the latter pair can only be explained by the different partition of each NBD-labeled lipid between the fluid phases, showing that NBD-DPPE is closer to t-PnA as compared to NBD-DOPE, and thus l_o phase should be in the vicinity of PCer/PSM domains. For the high X_{lo} range the trend of variation of E is independent on PCer content in all cases, showing that Chol abolished the effect of PCer.

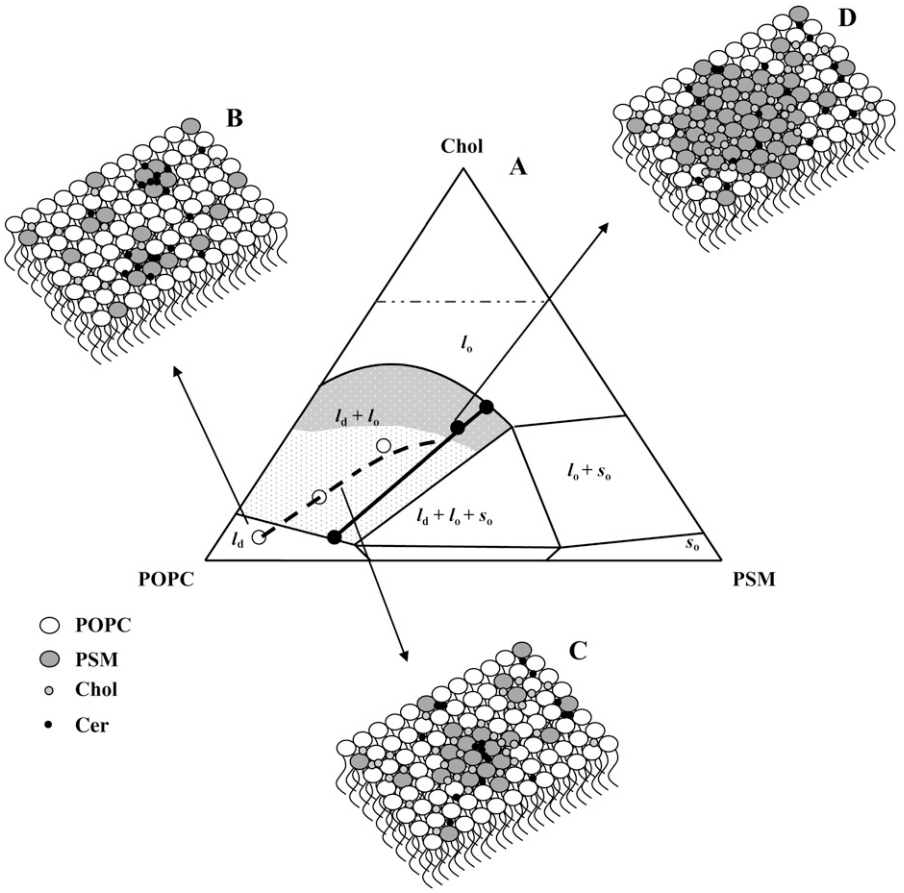

FIGURE 7 Schematic representation of the effect of PCer in lipid rafts biophysical properties and organization. (*A*) By recruiting PSM, PCer changes the composition of the mixtures and consequently the position of the tie line of the remaining fluid phase. The dashed black line and the white dots correspond to the estimated composition of the fluid phase that remains after the sequestering of PSM for gel-domain formation (see text for details). When increasing Chol content, the effect of PCer is opposed and less PSM is recruited for domain formation until 25%–33% Chol is reached and gel-domain formation completely abolished. Thus, the line that defines fluid phase composition should connect with the tie line in this region. According to this model, X_{lo} should decrease from 26% and 58% to 21% and 54%, respectively, when 4% PCer is present. (*B*) For the 100% l_d phase one PCer molecule recruits up to three PSM molecules and forms highly ordered PCer/PSM-gel domains. The amount of gel formed is considerable, $X_G \sim 15\%$, but the size of the domains is small, ~4 nm (see Discussion). Panels *B*, *C*, and *D* are a pictorial top view of the bilayer because ~250 molecules should be involved in the formation of a nanodomain of this dimension. (*C*) In the low-to-intermediate X_{Chol}, i.e., in the range of small sized rafts, PCer/PSM-gel domains are still present and are surrounded by lipid rafts (l_o phase). FRET experiments show that PCer is not forming platforms or promoting the coalescence of the small rafts into large ones. (*D*) In the high Chol, large sized rafts range, PCer ability to form gel domains with PSM is abolished by the presence of Chol that competes for the association with PSM. In this situation, lipid rafts are governing membrane properties.

It was previously suggested that Cer and Chol compete for association with raft lipids (21). However, in this study this competition is shown directly in a raft model system containing PSM. In addition, the effect is demonstrated at the level of the bilayer order, including the formation of highly ordered PCer/PSM-rich gel domains, thermotropic behavior, and lateral organization of the system.

DISCUSSION

PCer-induced perturbations on the biophysical properties of rafts: biological implications

We have shown previously that PCer is able to promote gel-fluid phase separation in binary POPC/PCer vesicles and drive the formation of large platforms. These gel platforms were highly ordered, excluding fluorescent probes that usually are able to partition into gel domains (20). Therefore, to draw meaningful conclusions based on the lipid phase-related properties of the probes, a partition study should always be performed for the particular system concerned. To better understand how the formation of Cer in rafts modulates the biophysical properties of the membranes, we selected a set of fluorescent probes, which were shown to partition differently between the coexisting phases under study (Table 1). Rafts, defined as l_o regions coexisting with an l_d phase, might have different compositions depending on the Chol and SM content. In biological membranes the Chol and SM content vary and, as a consequence, the size and properties of the rafts are also different (24). Thus, the biophysical changes induced by Cer should also depend on membrane composition. The comparison between the photophysical parameters of the probes in the model rafts showed that PCer strongly changed the properties of the membranes in the low-to-intermediate Chol/PSM regime, i.e., when the X_{lo} is low and rafts are small (Fig. 1). t-PnA fluorescence properties (both fluorescence anisotropy (Fig. 2 *A*) and fluorescence lifetime (Figs. 3 and 4 *A*)) clearly show that PCer induces the formation of a gel phase. Interestingly, the ability of PCer to form gel domains in these ternary mixtures is higher when compared to the effect that PCer had upon the properties of the fluid POPC vesicles (20). It can be safely concluded that

the effect of PCer is enhanced by the presence of PSM, driving the formation of PCer/PSM-rich gel domains. Further evidence arises from the change in the t-PnA fluorescence anisotropy as a function of temperature in the ternary mixtures, where the addition of PCer shifted the main transition of PSM-rich domains to higher temperatures (Fig. 5). The gel fraction formed by PCer in raft mixtures at 23°C can be estimated from the variation in the mean fluorescence lifetime of t-PnA (Fig. 4 *A*). Using Eq. 2 and the photophysical parameters of t-PnA in pure gel and fluid phases (20), we obtain $X_G \cong 0.02$ and $X_G \cong 0.15$ for 2 and 4 mol % PCer, respectively.

In opposition to t-PnA, DPH anisotropy (Fig. 2 *A*) only slightly changed with PCer content. Assuming that DPH behaves as usual (32), i.e., is able to partition equally between gel and fluid phases ($K_p^{g/f} \sim 1$), then for the situation where $X_G \cong 0.15$, and using $\langle r \rangle_G = 0.30$ (23), the expected anisotropy for DPH is $\langle r \rangle \sim 0.18$ (Eq. 4). The lower experimental value obtained ($\langle r \rangle = 0.15$) clearly reveals that even for low PCer concentrations DPH is excluded from the gel domains. This further suggests that PCer/PSM-rich gel domains are highly ordered, presenting biophysical properties similar to the ones observed for PCer-rich gel domains in POPC/PCer mixtures (20). For the situation where $X_G \cong 0.02$ the expected anisotropy for DPH is $\langle r \rangle \sim 0.15$, which is similar to the experimental value. The gel fraction formed by 2% PCer is very low and close to the boundary that separates the fluid from the gel-fluid coexistence in the binary diagram (20). In these conditions, PCer is mainly dispersed in the fluid ternary mixtures but promotes an increase in the order of the bilayer. As a consequence the photophysical parameters of the probes are not as sensitive to the presence of PCer as for 4 mol %. It should be stressed, however, that t-PnA is still able to detect an increase in the order of the membrane due to the strong increase in its quantum yield upon ordering of the acyl chain region. Interestingly, the ordering effect that 2% PCer has in the membrane in the l_d phase is equivalent to the effect of 25% Chol.

For lipid mixtures containing higher X_{lo} and larger rafts (Fig. 1), i.e., higher Chol content ($X_{Chol} > 33\%$), the presence of low PCer amounts did not markedly change the properties of the mixtures. In fact, the photophysical parameters of the probes, both fluorescence anisotropy and lifetime (Figs. 2 and 4), became independent of PCer content for X_{Chol} higher than ~25–33%. Moreover, this was independent on the preferential partition of the probes, showing that the PCer-induced biophysical changes in the rafts were completely abolished by the higher Chol amounts. Furthermore, the gel-fluid phase transition detected by t-PnA anisotropy (Fig. 5 *C*) was also eliminated in those mixtures.

Altogether, these data show that Chol and Cer compete for association with SM, driving the formation of distinct phases (l_o and gel, respectively) with different biophysical properties that might play opposite roles in the modulation of cellular processes. The mechanisms of Cer-dependent activation of cellular processes are still unclear, but evidence points to an indirect action through the modulation of the biophysical properties of the plasma membrane (12). Therefore, the alterations undergone in rafts by the generation of Cer might be a ruling factor in those processes.

PCer recruits PSM to form highly ordered gel domains

The effects that low amounts of PCer have upon the biophysical properties of the ternary mixtures are enormous, especially when compared to the same concentrations of PCer in binary systems. The presence of PSM in the ternary mixtures strongly enhanced the effect of PCer. This, together with the changes induced by PCer on the thermotropic properties of the mixtures and the opposite behavior of PCer and Chol in the modulation of the phase properties, confirms the association between PCer and PSM to form highly ordered gel domains that have similar biophysical properties to the PCer-gel domains (20). Moreover, the gel fraction induced by 4% PCer is considerable ($X_G = 0.15$) and cannot be solely due to PCer. The simplest approach to estimate the ability of PCer to recruit PSM molecules is to consider that all PCer present is participating in the formation of gel domains. In this way, 11 mol % PSM is required to obtain the total amount of gel. Note that this corresponds to ~50% total PSM present in the ternary mixtures in the low Chol/PSM regime. In these conditions, ~75% of the gel is composed of PSM, meaning that each PCer molecule is able to recruit two to three PSM molecules (this is the minimum value because we considered in these calculations that all PCer is in the gel, but some PCer might be still soluble in the fluid). These simple estimations are further confirmed by the depolarization of Rho-DOPE fluorescence in the presence of PCer (Fig. 2 *B*). Applying the model of Snyder and Freire (33) for the predicted depolarization as a function of surface density, we can relate the depolarization of Rho-DOPE in the presence and absence of PCer to the decrease in the available area for Rho-DOPE distribution. In the presence of 4% PCer, the surface area reduction for Rho-DOPE distribution necessary to account for the experimental depolarization is ~9%, which corresponds to ~5.1Å^2 per molecule reduction in the total area (60.6 Å^2 per molecule in l_d (24)). Calculating the corresponding area of PSM that is involved in gel-domain formation (using 47.8 Å^2 per SM molecule (34)), we obtain 5.2 Å^2. The similarity between the obtained values confirms our model for PCer ability to recruit up to three molecules of PSM. A very recent study of the Cer effects on raft mixtures containing DOPC (1,2-dioleoyl-*sn*-glycero-3-phosphocholine)/Chol/SM also suggests the formation of a gel phase most likely composed of Cer and SM, but as the authors state, further evidence is required to confirm the composition of this phase (35). Our study clearly demonstrates the enhanced interaction between these two lipids in the formation of a highly ordered gel phase.

The presence of increasing amounts of Chol in the ternary mixture opposes the effect of PCer, showing that in the case of the model systems here used, PCer is recruiting preferentially PSM in the l_d phase to form the gel domains. The effect of Chol is more pronounced when rafts are bigger and more PSM is involved in the formation of the l_o phase. In these conditions, PCer ability to recruit PSM molecules is abolished and the membrane biophysical properties are governed by lipid rafts. However, in cells Cer is generated in the plasma membrane within lipid rafts (which are considered small entities (36)) where the competition between the colocalized Cer and Chol should lead to a severe reorganization of the membrane domains where Cer is produced.

PCer/PSM domains are small and surrounded by rafts

It is often considered that Cer is able to drive the formation of large membrane platforms that might serve as sorting devices for signaling pathways (14,16). However, the lipid composition, the biophysical properties, and the size of such platforms are largely unknown. We have shown that in POPC/PCer binary mixtures PCer is able to drive the formation of large and highly ordered gel platforms (20). However, in more complex lipid mixtures already presenting fluid-fluid phase separation, the lipid structural organization induced by Cer might be different: it may completely segregate and form gel platforms with SM or promote the coalescence of small lipid rafts into larger domains but may also form small scattered gel domains. Application of state-of-the-art FRET methodologies to the systems under study allowed us to resolve some of these topological questions. Three situations were explored: i) $l_o - l_d$ phase separation; ii) gel $- l_o$ phase separation (the so-called Cer-platforms and lipid rafts, respectively); and iii) gel-fluid ($l_o + l_d$) phase separation. The probes used for donor and acceptor pairs were chosen according to their preferential partition into different phases (Table 1). A variation in the organization of the phases is directly related to a parallel change in FRET efficiency. From Fig. 6 where E is plotted as a function of X_{lo} for the three pairs, several conclusions arise: i) PCer affects the distribution of the lipids only in the low-to-intermediate Chol range (i.e., $X_{Chol} < 25$–33 mol %). ii) PCer promotes gel-fluid phase separation as reflected by the increase in E in the presence of PCer for the pair NBD-DPPE/Rho-DOPE (Fig. 6 *A*). The formation of a gel-rich phase results in the exclusion of the probes (both have preferential partition to the fluid phases), leading to a closer distribution. For the 100% l_d sample it is possible to predict approximately the expected increase of E in the presence of 4 mol % PCer. When 11 mol % PSM is sequestered from the fluid to the PCer/PSM domains, as shown above, the corresponding increase in E is only due to an increased surface acceptor concentration in the fluid. For a random probe distribution (see Appendix for the detailed model) the increase is calculated to be from 46% to 54%, in good agreement with the experimental value (Fig. 6 *A*), further confirming our model of up to three PSM molecules sequestered. In addition, for this pair, E decreases with the increase in X_{lo} because larger rafts are forming (24). We have thus direct evidence that PCer is not inducing coalescence of small rafts, because otherwise E would not increase with PCer for lower X_{Chol}. This is further confirmed by applying the same model for the calculation of E. Considering that for low X_{lo} (~26%), PCer's ability to form gel domains is the same as in 100% l_d and taking into account the presence of small raft domains, the expected increase in E due to the decrease in the fluid area for probe distribution is from 42% in the absence of PCer to 47% in the presence of 4% PCer, similarly to the observed experimental values (Fig. 6 *A*), clearly revealing that raft size remains unchanged in the presence of PCer. Different cellular processes are activated by raft coalescence and by Cer formation. If Cer biological action is, in fact, related to the biophysical changes that it causes in the lipid bilayer, it seems reasonable that raft reorganization induced by Cer is different from the reorganization that takes place in Cer-independent processes. Ganglioside G_{M1}, for example, has a completely different effect on rafts. In small amounts it hardly changes the order of the bilayer, but 4 mol % is able to increase the size of the small rafts, as shown by a decreased E between NBD-DPPE and Rho-DOPE (24). iii) E decreases for both t-PnA/NBD-DPPE and t-PnA/NBD-DOPE in the presence of PCer as a consequence of gel-domain formation. For these pairs E increases with X_{lo}. This latter effect results from the increase in quantum yield of t-PnA and therefore the Förster radius, R_o, as it partitions to more ordered phases. It should be stressed that t-PnA quantum yield and thus R_0 for these pairs also increased with PCer. An increase in R_0 should lead to a higher E; however, FRET efficiency decreases in the presence of PCer indicating that the separation distance between the donors and the acceptors is increasing, and thus gel domains that exclude the acceptors are forming.

For these situations, the variation in E along the tie line is due not only to a change in the size of the domains, but also to the variation of R_0 and determination of domains size is complex. In addition, a three-phase situation is present (see below), and modeling this scenario would require approximations too severe. Nevertheless, the high difference obtained for energy transfer from t-PnA to NBD-DOPE and NBD-DPPE gives important information about the organization of lipid domains. Due to the higher decrease in E we can conclude that the distance that separates t-PnA from NBD-DOPE is higher as compared to NBD-DPPE, showing that the l_o phase should be closer to PCer/PSM-rich gel domains as compared to the l_d phase. It should be stressed that comparison between the two FRET pairs cannot be made in relation to the absolute E values, but to the trend of variation of E in the presence and absence of PCer. This is because E is dependent on acceptor concentration, which was different for the two FRET pairs. Nevertheless, to ensure that the

obtained profiles are not related to the differences in the acceptor concentration, the expected E for a donor-acceptor random distribution both in the 100% l_d and 100% l_o phases was determined for these pairs (see Appendix). The values obtained are 32% and 15% in the l_d phase and 59% and 41% in the l_o phase for t-PnA/NBD-DPPE and t-PnA/NBD-DOPE, respectively. These values are in good agreement with the experimental ones (Fig. 6, *B* and *C*), showing that E in the pure phases is in fact reflecting the random distribution of both donors and acceptors.

These results indicate that PCer is able not only to change the biophysical properties of the small rafts driving the formation of PCer/PSM-rich gel domains, but also to reorganize the lipids in the membrane, being preferentially closer to the l_o domains (see below). This type of organization is expected on the basis of interfacial tension arguments. In fact, due to its intermediate properties in between gel and l_d phases, l_o domains surrounding gel would act as a wetting layer, decreasing surface tension and stabilizing the interfaces (37). This would also prevent the rapid growth of domains, explaining the absence of raft coalescence and large PCer platform formation. Note that the experimental data unequivocally show that in the presence of PCer and in the low-to-intermediate Chol range three phases must be present: a) The PCer-rich gel phase is detected by t-PnA photophysical parameters that are a fingerprint for this phase (Figs. 2 *A*, 3, and 4 *A*) and in addition, from the anisotropy of NBD-DOPE and Rho-DOPE (Fig. 2 *B*) that decreases as a consequence of the increased depolarization due to the exclusion of the probes from these domains; b) The PSM/Chol-rich l_o phase is detected from DPH anisotropy which is typical of this phase both in the presence and absence of PCer. Since DPH is excluded from PCer-rich gel, if only gel and l_d phases were present, then DPH anisotropy should decrease in the presence of PCer. On the contrary, if only the gel and l_o phases were present then DPH anisotropy should increase toward values identical to those obtained with higher Chol content; c) The anisotropy trend of variation of DPH, NBD-DOPE, NBD-DPPE, and Rho-DOPE is identical in the presence and absence of PCer and because all these probes are excluded from PCer-rich gel domains, it indicates that the remaining fluid phase should present l_o/l_d phase coexistence similarly to the mixtures in the absence of PCer; and d) If only two phases, i.e., gel and fluid (without l_o/l_d coexistence) were present then E between NBD-DPPE/Rho-DOPE should remain invariant in the low-to-intermediate Chol range when 4% PCer is present. Both probes are excluded from PCer-rich gel domains and a random distribution in the remaining fluid phase (assuming that l_d/l_o phases were not coexisting) should give an E value identical to the one obtained for the 100% l_d mixture. Moreover, assuming the same situation, FRET between t-PnA/NBD-DPPE and NBD-DOPE should result in identical profiles because only a simple situation of energy transfer from a gel to a fluid phase would occur. Only the presence of three phases, gel, l_o, and l_d can result in the experimentally observed profiles of variation for the different FRET pairs and also anisotropy and lifetime profiles. To further support our evidence, recently it was observed that the presence of three phases in a different type of raft-like mixtures containing higher amounts of Cer by combined atomic force microscopy, fluorescence imaging, and fluorescence correlation spectroscopy (35). The authors observed that three phases were present in mixtures containing 1:1:1 DOPC/Chol/(SM + Cer) only for Cer $>$ 8% total lipid, whereas 4% Cer was not able to induce changes in the lipid lateral organization. Note that these results are not in contradiction to our observations because for equivalent mixtures as the ones used by the authors, i.e., for mixtures containing ~33% Chol, which in our work correspond to the high Chol/PSM range, PCer effects are abolished by Chol. The thorough study performed here clearly indicates that the effects that Cer has upon the biophysical properties and lipid lateral organization in the membrane cannot be generalized and the exact membrane lipid composition must be known before relating the Cer-induced biophysical changes and the activation/inhibition of cellular processes.

In terms of domain size, it can be safely stated that the size of the fluid domains is not significantly changed by PCer (as explained above). In this scenario, where rafts are surrounding the PCer/PSM domains, for the rafts to remain small, it is mandatory that the gel domains inside also be quite small. Thus, we do not have any evidence for the Cer-induced formation of large platforms in raft-containing systems at least up to 4 mol % PCer. Using again the 100% l_d sample, the size of the PCer/PSM domains can be estimated (both from t-PnA/NBD-DPPE and t-PnA/NBD-DOPE pairs). Taking advantage of the complete exclusion of the acceptors from the gel domains, the contribution to total E from donors located in those domains can be calculated assuming that these donor molecules are transferring to acceptors in the fluid phase, separated by an exclusion radius for acceptors R_e, which corresponds to the size of the gel domains (see Appendix for a detailed model). The model for FRET with randomly distributed acceptors and an exclusion radius has analytical solution (38), and by introducing different R_e values in the model, the experimental E will be reached. In this way, we obtained a value of ~3.8 and ~4.0 nm for the size of the PCer/PSM domains, determined from t-PnA/NBD-DPPE and t-PnA/NBD-DOPE pairs, respectively. The similarity between the two values further indicates that the trend of E variation is not dependent on acceptor concentration, and thus the differences in the profiles are reflecting the PCer-induced lateral reorganization.

Additional information can be obtained from FRET between t-PnA and NBD-DOPE. These two probes partition evenly between coexisting l_o and l_d phases (both $K_p^{lo/ld} \sim 1$), and thus a random distribution of donors and acceptors for energy transfer can always be assumed. In the absence of PCer the increase in E is due to the reduction in the surface area for probe distribution due to the condensation effect of

Chol and to an increase in the donor quantum yield and consequently in R_0 for the donor-acceptor pair. In the presence of PCer domains E is the result of the donors that are located both in gel and fluid phases (see Appendix) transferring to the acceptors that are randomly distributed in the fluid phase. The FRET efficiencies expected assuming a situation where PCer is always able to recruit 11 mol % PSM for the formation of ~4 nm gel domains are plotted in Fig. 6 *C*. The similarity between the theoretical and experimental values in the low Chol range clearly indicates that PCer is able to recruit PSM for gel domain and that the predicted size for these gel domains remains invariant in this range of Chol content. However, the experimental E increases with Chol content, in contrast to the value calculated taking into account PCer domain formation, showing that PCer domains are destroyed by high amounts of Chol. Note that this pair is insensitive to l_o/l_d phase separation (since both probes partition equally among these phases) and thus is only reporting the existence of gel domains.

The same type of analysis for the t-PnA/NBD-DPPE pair is more complex because partition among three phases should be considered, and the different contributions to E would depend on the donor in the gel and in the fluid transferring for acceptors predominantly in the l_o phase but also in the l_d phase. Nevertheless, using identical conditions as the ones applied for the t-PnA/NBD-DOPE pair further evidence is obtained for the suggested model of lipid lateral organization of the rafts in the presence of PCer. The expected E for PCer gel-domain formation is plotted in Fig. 6 *B*. The higher experimental values in the low Chol range clearly indicate that i) acceptors are not randomly distributed in the fluid phase, probing the existence of fluid-fluid phase separation; and ii) the l_o phase is closer to gel domains, otherwise FRET efficiency would not be so much higher than the calculated value assuming random distribution of acceptors in the fluid because the surface density of NBD-DPPE is much higher in the l_o phase due to its partition coefficient. To further confirm that the l_o phase is closer to PCer/PSM-rich gel domains as compared to the l_d phase, FRET efficiency was calculated assuming two situations: a) only the l_d phase is surrounding PCer/PSM-rich gel domains, and b) only the l_o phase is surrounding PCer/PSM-rich gel domains. In these calculations it was assumed that the donor in the gel phase was not able to transfer to the l_o or to the l_d phase, respectively, and the surface density of the acceptors in each fluid phase and the size of gel domains were taken into account (see Appendix). This type of analysis can only be made in relation to the situation where PCer recruits PSM for the formation of small gel domains, i.e., for the low Chol range. The obtained values for E (Fig. 6 *B*) clearly show that if only the l_d phase were nearby gel domains, which would not be surprising taking into account the amount of this phase in this mixture (~74%), FRET efficiency would be lower and close to the situation where acceptors are randomly distributed in the fluid phases. On the contrary, if only the l_o phase were surrounding gel domains, then the expected E would be higher than the experimental value. However, these results do not indicate that gel domains are not surrounded by the l_o phase. In fact, the experimental value is closer to the theoretical value assuming energy transfer from the gel to the l_o phase (situation b) as compared to the l_d phase (situation a), suggesting that gel domains are at least in part surrounded by l_o domains. This is indeed the case because the amount of the l_o phase in this mixture is not enough to completely surround the PCer/PSM-rich gel domains. Taking into account the dimensions of the gel domains (~4 nm), at least 250 molecules are required to form these nanodomains. Moreover, the amount of gel phase present in this mixture (~15%) implies that ~275 gel nanodomains per vesicle should be present. The minimum number of molecules required to surround these nanodomains (considering that only one layer of molecules is involved) is ~1200, i.e., 4–5 times more molecules in the l_o phase (compared to the ones involved in gel-domain formation) are required to surround all the gel domains. Thus, for ~15% of gel, at least 60% of l_o phase is required. For the mixture in question, only 26% of the l_o phase is present, which is not enough to cover all the gel. Nevertheless, we can clearly state that part of the gel domains are surrounded by rafts because otherwise FRET efficiency would be lower. Moreover, the amount of the l_d phase is three times higher than the l_o phase, but the experimental E value is closer to the theoretical E value assuming that the t-PnA in the gel is transferring only to the l_o phase, which implies that in fact all the l_o domains should be in the vicinity of gel domains. This type of organization is in agreement with recent results showing that Cer domain formation takes place inside or close to the boundaries of the SM-rich l_o phase (35).

Altogether these results show that PCer-induced changes are complex both in phase behavior and lipid lateral distribution and strongly dependent on the lipid composition of the rafts. Moreover, PCer per se is not able to induce neither the formation of large platforms in raft model membranes nor the coalescence of rafts. However, it strongly changes the biophysical properties of the membranes, inducing the formation of small gel nanodomains. The size of such domains is in agreement with those expected for a raft domain in a resting cell. In fact, studies not involving cross-linking methods have shown that raft domains should be smaller than 10 nm, and additional mechanisms (such as those activated under stimulation) of domain stabilization are required for the formation of larger domains (reviewed in Kusumi and Suzuki (39)).

CONCLUSIONS

This study has lead to a significant number of relevant conclusions, with implications at different levels.

From the methodological point of view, the correct biophysical characterization of biologically relevant lipid mixtures should be performed in a stepwise fashion. The previous thorough studies of the ternary system POPC/PSM/Chol and of

the binary system POPC/PCer were crucial. As the complexity of the system is increased, the importance of using multiple fluorescent probes, and different FRET pairs, with a well-defined lipid-phase behavior becomes more and more essential.

From a biophysical perspective, striking results were obtained. Low amounts of PCer have a remarkable effect on the bilayer order, and the effect of PCer is amplified by the presence of PSM. For example, the formation of gel domains occurs for much lower PCer content than when it is mixed only with POPC. Also striking is the ability of Cer to recruit up to three SM molecules, forming a highly compact gel that excludes most fluorescent probes. The small size of these domains as compared to the PCer domains in the binary system (20) and the ability of PCer/PSM domains to be surrounded by rafts are other important conclusions reached in this study.

Some clarification should be made concerning lipid domain terminology. For example, the term ''Cer platforms'' is often encountered, implicitly stating that these are big domains. We have shown here that this is not the case for lipid mixtures mimicking the outer leaflet of mammalian plasma membranes. Sometimes they are called (Cer) rafts, but lipid rafts are rich in Chol and are l_o domains, whereas Cer/SM domains should be in a gel-like phase and exclude Chol.

From the biological point of view, the nature of the Cer/SM domains suggests exclusion of other membrane components, like proteins, rather than their inclusion. The competition between Chol and Cer for SM association suggests that when Cer is formed in lipid rafts a severe lateral reorganization should occur. This could be related to a triggering of apoptosis that would be controlled by a Chol/Cer ratio. In this work we show that up to 2 mol % PCer (that should be in the range of Cer levels in resting cells) Cer hardly segregates into gel domains and does not recruit SM. Upon apoptotic stimuli Cer can reach 10% of total lipid in living cells (40), and as low as 4 mol % PCer is enough to affect the membrane properties in a completely different manner. In cells with plasma membrane particularly rich in Chol (higher than ~25–30%) this can be a protection from triggering of apoptosis by Cer. The ability of Cer to recruit more than one SM molecule also suggests that when Cer is generated in the membrane in response to stress stimulus, an amplification mechanism of SMase activity may take place which, in turn, would rapidly lead to the activation of signaling cascades and/or processes leading to cell death, such as apoptosis.

APPENDIX: MODELS FOR THE DETERMINATION OF THEORETICAL FRET EFFICIENCY AND PCER/PSM GEL DOMAIN SIZE

For the t-PnA/NBD-DPPE and t-PnA/NBD-DOPE pairs, the location of the chromophores in the bilayer (bilayer center and membrane surface for donor and acceptor, respectively) only allows out-of-plane energy transfer (*trans*) and the model that describes FRET with randomly distributed donor (t-PnA) and acceptor (NBDs) molecules, assuming a radius of exclusion of acceptors (R_e) around the donor, is given by de Almeida et al. (24):

$$\rho_{trans}(t) = \exp\left\{ -\frac{2c}{\Gamma(2/3)\times b}\int_0^{w/\sqrt{w^2+R_e^2}} [1 - \exp(-t\,b^3\,\alpha^6)]\,\alpha^{-3}\int d\alpha \right\}, \quad \text{(A1)}$$

where

$$c = \Gamma(2/3)\times n\times \pi \times R_0^2 \times \bar{\tau}^{-1/3}. \quad \text{(A2)}$$

In this equation, n is the surface density of acceptors, R_0 is the Förster radius, R_e is the exclusion radius, Γ is the complete γ function, $b = (R_0/w)^2/\bar{\tau}^{1/3}$, and w is the interplanar donor-acceptor distance. In the calculation of the surface density of acceptors, an area per molecule of 66.4 Å^2 for POPC (41), 47.8 Å^2 for PSM (34), and 37.7 Å^2 for Chol (42) were considered. The condensation effect of Chol was taken into account (42). $R_0 = 25$ Å and $R_0 = 29$ Å, for both D/A pairs in pure l_d and l_o phases, respectively, is not small compared to the membrane thickness, and transfer to the two leaflets occurs. In this situation, the donor decay in the presence of acceptor is given by

$$i_{DA}(t) = i_D(t)\rho_{trans1}(t)\rho_{trans2}(t), \quad \text{(A3)}$$

where $w_1 = 12.1$ Å (28) was used for FRET in the same leaflet for both l_d and l_o phases and $w_2 = 27.9$ Å and $w_2 = 36.9$ Å (24) were used for FRET in the opposite leaflet for l_d and l_o phases, respectively. FRET efficiency, E, is computed numerically using the relation $E = 1 - \bar{\tau}_{DA}/\bar{\tau}_D$. For the 100% l_d and 100% l_o samples in the absence of PCer, only the fluid phase is present and $R_e = 0$, yielding an E value equal to the one obtained experimentally, $E \sim 31\%$ and $E \sim 15\%$ in the l_d phase and $E \sim 59\%$ and $E \sim 41\%$ in the l_o phase for t-PnA/NBD-DPPE and t-PnA/NBD-DOPE pairs, respectively (Fig. 6, *B* and *C*).

If phase separation occurs, the donor decay in the absence of acceptors is given by

$$i_D(t) = x_1 i_{D1}(t) + x_2 i_{D2}(t), \quad \text{(A4)}$$

where x_i is the mol fraction and $i_{Di}(t)$ the fluorescence decay of the donor in phase $i = 1,2$. When the domains are big enough to prevent significant FRET from donor in one phase to acceptors in a different phase, the donor decay in the presence of acceptor is given by

$$i_{DA}(t) = x_1 i_{D1}(t)\rho_{trans1,1}(t)\rho_{trans2,1}(t) + x_2 i_{D2}(t)\rho_{trans1,2}(t)\rho_{trans2,2}(t), \quad \text{(A5)}$$

where $\rho_{trans,i}(t)$ are calculated as for the one phase situation but taking into account the parameters of each phase.

Equations A4 and A5 were also used to determine the size of gel domains that are formed in the presence of 4 mol % PCer. In this particular case, those equations are valid even if the Cer gel domains are small, because the acceptor in totally excluded from these domains. Thus, only FRET from the gel to the fluid and FRET within the fluid take place, for which t-PnA concentration in the gel together with an exclusion radius, and t-PnA concentration in the fluid without exclusion radius, and t-PnA concentration in the fluid without exclusion radius are used, respectively. It was considered that 11% PSM is recruited for gel-domain formation, and the size of these domains is given by the R_e that is required to obtain the experimental $E \sim 25\%$ and $E \sim 12\%$ (because PCer-rich domains exclude the acceptors), resulting in $R_e \sim 3.8$ and $R_e \sim 4$ nm for t-PnA/NBD-DPPE and t-PnA/NBD-DOPE pairs, respectively. To determine the expected E for a situation where PCer gel domains were always formed (independently of lipid raft composition), a random distribution of the probes in the fluid phase was assumed and X_G was set to 15% (as determined from t-PnA lifetime measurements) and $R_e = 3.8$ and 4.0 nm for t-PnA/NBD-DPPE and t-PnA/NBD-DOPE, respectively.

These equations were also used to determine the FRET efficiency between t-PnA/NBD-DPPE for a situation where gel domains were surrounded only by the l_d or l_o phase. In these calculations it was assumed that t-PnA in the gel phase was only able to transfer to one of the phases (the phase that was considered to be surrounding the gel domains), whereas t-PnA in the fluid phase was able to transfer both to the l_d and l_o phases (as in the situation of PCer absence). The amount of gel phase, the partition of t-PnA into the gel phase, and the surface density of the acceptors in each of the fluid phases were taken into account. Exclusion of the acceptors from the gel phase was assumed, and R_e was set to 3.8 nm.

The FRET model for random distribution of the NBD-DPPE/Rho-DOPE Förster pair was described in detail previously (24). Since both chromophores are located in the bilayer surface, both in-plane (*cis*) and out-of-plane (*trans*) energy transfer occur and the donor decay in the presence of acceptor is given by

$$i_{DA}(t) = i_D(t)\rho_{cis}(t)\rho_{trans}(t), \tag{A6}$$

where,

$$\rho_{cis}(t) = \exp\left\{-\pi R_0^2 n\gamma\left[\frac{2}{3}, \left(\frac{R_0}{R_e}\right)^6 (t/\bar{\tau})\right](t/\bar{\tau})^{1/3} + \pi R_e^2 n\left(1 - \exp\left[-\left(\frac{R_0}{R_e}\right)^6 (t/\bar{\tau})\right]\right)\right\} \tag{A7}$$

and

$$\gamma(x, y) = \int_0^y z^{x-1}\exp(-z)dz \tag{A8}$$

is the incomplete γ function.

For the 100% l_d sample in the absence of PCer, the total area per molecule available for acceptor distribution is 60.6 Å^2 (24), and the calculated E is in good agreement with the experimental one (~46%). When 4% PCer is present and 11% PSM is sequestered (corresponding to a reduction of 5.2 Å^2 per molecule), gel domains that exclude the probes are formed. The calculated E value assuming the reduction in the available area for probe distribution is similar to the experimental one (~54%), confirming the model for PSM sequestering by PCer. In the presence of low Chol amounts (X_{lo} = 0.26) it was assumed that PCer was able to recruit up to three PSM molecules for gel-domain formation. Taking into account the presence of small raft domains (<20 nm) (24), the calculated E due to a reduction in the area is ~47%, identical to the experimental value showing that PCer is not inducing the coalescence of these small rafts.

This work (POCTI/QUI/57123/2004) was supported and research grants (BD/10029/2002 to L.C.S., BPD/17842/2004 to R.F.M. de A., and BPD/11488/2002 to A.F.) were given by Programa Operacional ''Ciência, Tecnologia e Inovação''/Fundação para a Ciência e Tecnologia, Portugal.

REFERENCES

1. Kusumi, A., C. Nakada, K. Ritchie, K. Murase, K. Suzuki, H. Murakoshi, R. S. Kasai, J. Kondo, and T. Fujiwara. 2005. Paradigm shift of the plasma membrane concept from the two-dimensional continuum fluid to the partitioned fluid: high-speed single-molecule tracking of membrane molecules. *Annu. Rev. Biophys. Biomolec. Struct.* 34:351–378.
2. Karnovsky, M. J., A. M. Kleinfeld, R. L. Hoover, E. A. Dawidowicz, D. E. McIntyre, E. A. Salzman, and R. D. Klausner. 1982. Lipid domains in membranes. *Ann. N. Y. Acad. Sci.* 401:61–75.
3. Estep, T. N., D. B. Mountcastle, Y. Barenholz, R. L. Biltonen, and T. E. Thompson. 1979. Thermal behavior of synthetic sphingomyelin-cholesterol dispersions. *Biochemistry.* 18:2112–2117.
4. Ipsen, J. H., G. Karlstrom, O. G. Mouritsen, H. Wennerstrom, and M. J. Zuckermann. 1987. Phase-equilibria in the phosphatidylcholine-cholesterol system. *Biochim. Biophys. Acta.* 905:162–172.
5. Sankaram, M. B., and T. E. Thompson. 1990. Interaction of cholesterol with various glycerophospholipids and sphingomyelin. *Biochemistry.* 29:10670–10675.
6. Sankaram, M. B., and T. E. Thompson. 1991. Cholesterol-induced fluid-phase immiscibility in membranes. *Proc. Natl. Acad. Sci. USA.* 88:8686–8690.
7. Almeida, P. F. F., W. L. C. Vaz, and T. E. Thompson. 1992. Lateral diffusion in the liquid phases of dimyristoylphosphatidylcholine/cholesterol lipid bilayers: a free volume analysis. *Biochemistry.* 31: 6739–6747.
8. Simons, K., and E. Ikonen. 1997. Functional rafts in cell membranes. *Nature.* 387:569–572.
9. Holthuis, J. C. M., G. van Meer, and K. Huitema. 2003. Lipid microdomains, lipid translocation and the organization of intracellular membrane transport (Review). *Mol. Membr. Biol.* 20:231–241.
10. Futerman, A. H., and Y. A. Hannun. 2004. The complex life of simple sphingolipids. *EMBO Rep.* 5:777–782.
11. Kolesnick, R. N., F. M. Goni, and A. Alonso. 2000. Compartmentalization of ceramide signaling: physical foundations and biological effects. *J. Cell. Physiol.* 184:285–300.
12. Cremesti, A. E., F. M. Goni, and R. Kolesnick. 2002. Role of sphingomyelinase and ceramide in modulating rafts: do biophysical properties determine biologic outcome? *FEBS Lett.* 531:47–53.
13. Shaul, P. W., and R. G. W. Anderson. 1998. Role of plasmalemmal caveolae in signal transduction. *Am. J. Physiol.* 19:L843–L851.
14. Gulbins, E., S. Dreschers, B. Wilker, and H. Grassme. 2004. Ceramide, membrane rafts and infections. *J. Mol. Med.* 82:357–363.
15. Bollinger, C. R., V. Teichgraber, and E. Gulbins. 2005. Ceramide-enriched membrane domains. *Biochim. Biophys. Acta.* 1746: 284–294.
16. Grassme, H., A. Riehle, B. Wilker, and E. Gulbins. 2005. Rhinoviruses infect human epithelial cells via ceramide-enriched membrane platforms. *J. Biol. Chem.* 280:26256–26262.
17. Holopainen, J. M., M. Subramanian, and P. K. J. Kinnunen. 1998. Sphingomyelinase induces lipid microdomain formation in a fluid phosphatidylcholine/sphingomyelin membrane. *Biochemistry.* 37:17562–17570.
18. Hsueh, Y. W., R. Giles, N. Kitson, and J. Thewalt. 2002. The effect of ceramide on phosphatidylcholine membranes: a deuterium NMR study. *Biophys. J.* 82:3089–3095.
19. Fidorra, M., L. Duelund, C. Leidy, A. C. Simonsen, and L. A. Bagatolli. 2006. Absence of fluid-ordered/fluid-disordered phase coexistence in ceramide/POPC mixtures containing cholesterol. *Biophys. J.* 90:4437–4451.
20. Silva, L., R. F. M. De Almeida, A. Fedorov, A. Matos, and M. Prieto. 2006. Ceramide-platform formation and -induced biophysical changes in a fluid phospholipid membrane. *Mol. Membr. Biol.* 23:137–148.
21. Megha, and E. London. 2004. Ceramide selectively displaces cholesterol from ordered lipid domains (rafts): implications for lipid raft structure and function. *J. Biol. Chem.* 279:9997–10004.
22. Sot, J., L. A. Bagatolli, F. M. Goni, and A. Alonso. 2006. Detergent-resistant, ceramide-enriched domains in sphingomyelin/ceramide bilayers. *Biophys. J.* 90:903–914.
23. de Almeida, R. F. M., A. Fedorov, and M. Prieto. 2003. Sphingomyelin/phosphatidylcholine/cholesterol phase diagram: boundaries and composition of lipid rafts. *Biophys. J.* 85:2406–2416.
24. de Almeida, R. F. M., L. M. S. Loura, A. Fedorov, and M. Prieto. 2005. Lipid rafts have different sizes depending on membrane composition: a time-resolved fluorescence resonance energy transfer study. *J. Mol. Biol.* 346:1109–1120.
25. Sklar, L. A., B. S. Hudson, M. Petersen, and J. Diamond. 1977. Conjugated polyene fatty-acids on fluorescent-probes—spectroscopic characterization. *Biochemistry.* 16:813–819.
26. Lentz, B. 1988. Membrane ''fluidity'' from fluorescence anisotropy measurements. *In* Spectroscopic Membrane Probes, Vol. 1. L. Loew, editor. CRC, Boca Raton, FL. 13–41.

27. Haugland, R. 1996. Handbook of Fluorescent Probes and Research Chemicals. Molecular Probes, Eugene, OR.

28. de Almeida, R. F. M., L. M. S. Loura, A. Fedorov, and M. Prieto. 2002. Nonequilibrium phenomena in the phase separation of a two-component lipid bilayer. *Biophys. J.* 82:823–834.

29. Loura, L. M. S., A. Fedorov, and M. Prieto. 2001. Fluid-fluid membrane microheterogeneity: a fluorescence resonance energy transfer study. *Biophys. J.* 80:776–788.

30. Prieto, M. J. E., M. Castanho, A. Coutinho, A. Ortiz, F. J. Aranda, and J. C. Gomezfernandez. 1994. Fluorescence study of a derivatized diacylglycerol incorporated in model membranes. *Chem. Phys. Lipids.* 69:75–85.

31. Lakowicz, J. 1999. Principles of Fluorescence Spectroscopy. Kluwer Academic, New York.

32. Lentz, B. R. 1989. Membrane fluidity as detected by diphenylhexatriene probes. *Chem. Phys. Lipids.* 50:171–190.

33. Snyder, B., and E. Freire. 1982. Fluorescence energy-transfer in 2 dimensions—a numeric solution for random and nonrandom distributions. *Biophys. J.* 40:137–148.

34. Li, X. M., J. M. Smaby, M. M. Momsen, H. L. Brockman, and R. E. Brown. 2000. Sphingomyelin interfacial behavior: the impact of changing acyl chain composition. *Biophys. J.* 78:1921–1931.

35. Chiantia, S., N. Kahya, J. Ries, and P. Schwille. 2006. Effects of ceramide on liquid-ordered domains investigated by simultaneous AFM and FCS. *Biophys. J.* 90:4500–4508.

36. Rao, M., and S. Mayor. 2005. Use of Forster's resonance energy transfer microscopy to study lipid rafts. *Biochim. Biophys. Acta.* 1746:221–233.

37. Simons, K., and W. L. C. Vaz. 2004. Model systems, lipid rafts and cell membranes. *Annu. Rev. Biophys. Biomolec. Struct.* 33:269–295.

38. Davenport, L., R. E. Dale, R. H. Bisby, and R. B. Cundall. 1985. Transverse location of the fluorescent-probe 1,6-diphenyl-1,3,5-hexatriene in model lipid bilayer-membrane systems by resonance excitation-energy transfer. *Biochemistry.* 24:4097–4108.

39. Kusumi, A., and K. Suzuki. 2005. Toward understanding the dynamics of membrane-raft-based molecular interactions. *Biochim. Biophys. Acta.* 1746:234–251.

40. Hannun, Y. A. 1996. Functions of ceramide in coordinating cellular responses to stress. *Science.* 274:1855–1859.

41. Chiu, S. W., E. Jakobsson, S. Subramaniam, and H. L. Scott. 1999. Combined Monte Carlo and molecular dynamics simulation of fully hydrated dioleyl and palmitoyl-oleyl phosphatidylcholine lipid bilayers. *Biophys. J.* 77:2462–2469.

42. Smaby, J. M., M. M. Momsen, H. L. Brockman, and R. E. Brown. 1997. Phosphatidylcholine acyl unsaturation modulates the decrease in interfacial elasticity induced by cholesterol. *Biophys. J.* 73:1492–1505.